

Supporting Information

for

Multiple Correlations Between Spin Crossover and Fluorescence in a Dinuclear Compound

Chun-Feng Wang,^{a,b} Ming-Jun Sun,^a Qi-Jie Guo,^a Ze-Xing Cao,^{*,a} Lan-Sun Zheng^a and Jun Tao^{*,a,b}

^aState Key Laboratory of Physical Chemistry of Solid Surfaces and Department of Chemistry,
College of Chemistry and Chemical Engineering, Xiamen University, Xiamen 361005, People's
Republic of China.

^bKey Laboratory of Cluster Science of Ministry of Education, School of Chemistry and Chemical
Engineering, Beijing Institute of Technology, Beijing 102488, People's Republic of China.

E-mail: taojun@xmu.edu.cn; zxcao@xmu.edu.cn; taojun@bit.edu.cn.

Table of Contents

1. Materials and Methods	S4
2. Syntheses	S4
3. Computational Methods	S5
4. Additional Tables	
Table S1 Elemental analyses	S8
Table S2 Crystal data and structure refinement	S8
Table S3 Comparison of bond lengths of experimental and theoretical data	S9
Table S4 Metal-ligand and metal-metal bond distances for optimized geometries of low-spin state of 1 using a great number of DFT functional, and the experimental values are also displayed. The temperature is set to 100 K	S9
Table S5 Metal-ligand and metal-metal average bond distances for optimized geometries of different spin states of 1 at the PBE1PBE/6-311G(d,p) level, and the experimental values are also shown. The calculated temperature is 300 K	S10
Table S6 The predicted excitation energies for the lowest 60 transitions of 1 in hs and ls states	S10
Table S7 Optimized geometry of 1 in the high-spin state	S12
Table S8 Optimized geometries of 1 in the low-spin state	S18
5. Additional Figures	
Fig. S1 Crystal structure of 1	S19
Fig. S2 Magnetic properties of 1	S19
Fig. S3 Fluorescent emission spectra of 1 and pnm at RT	S20
Fig. S4 T-dependent fluorescent spectra of pnm	S20

Fig. S5 T-dependent fluorescent spectra of 1	S21
Fig. S6 Experimental and theoretical spectra of 1 at hs state.....	S23
Fig. S7 Experimental and theoretical spectra of 1 at ls state.....	S24
Fig. S8 Molecular orbitals of $S_0 \rightarrow S_1$ transition for the hs state.....	S25
Fig. S9 Molecular orbitals of $S_0 \rightarrow S_1$ transition for the ls state.....	S26
Fig. S10 Theoretical electronic absorption spectrum of pnm.....	S27
Fig. S11 Optimized crystal structures of 1 in ls and hs states.....	S27
Fig. S12 Electron spin density of 1 in hs and ls states.....	S28
Fig. S13 Normalized diffuse reflectivity spectra of pnm.....	S38
Fig. S14 Normalized excitation and emission spectra of pnm.....	S29
5. References.....	S30

1. Materials and Methods

Ammonium thiocyanate and 4-NH₂-1,2,4-triazole were purchased from Aladdin and Alfa Aesar, respectively. Iron(II) chloride tetrahydrate and Benzaldehyde were obtained from Tianjin Chemical Reagent Company (China). Ascorbic acid and all solvents were purchased from Sinopharm Chemical Reagent Co., Ltd. All starting materials were used without further purification.

Solid-state emission spectra of fluorescence were measured on an Edinburgh FLS 980 fluorescence spectrophotometer. Absorbance spectra of the ligand were recorded on a Shimadzu UV2550 spectrophotometer with scan rate of 600 nm min⁻¹. Infrared spectra (KBr pellets) were recorded in the range of 400–4000 cm⁻¹ on a Nicolet 5DX spectrometer. Elemental analyses for C, H, N and S were performed on a Vario EL III elemental analyzer. Diffuse reflectance spectra (DRS) were obtained with a Varian Cary 5000 UV–Vis spectrometer with scan rate of 600 nm min⁻¹ using BaSO₄ as a reference. Magnetic measurements were carried out on a Quantum Design MPMS XL7 magnetometer working in the 2–300 K temperature range with 1 K min⁻¹ sweeping rate under a magnetic field of 5000 Oe. The solid-state fluorescence and magnetic properties were measured on fresh crystalline samples with a drop of mother liquor.

2. Syntheses

(E)-phenyl-N-(4H-1,2,4-triazol-4-yl)methanimine (pnm): 4-NH₂-1,2,4-triazole (2.100 g, 24.0 mmol) was dissolved in 20 mL ethanol and benzaldehyde (2.547 g, 24.0 mmol) was added, then the mixture was refluxed for 5 h. The reaction solution was then left undisturbed at room temperature

for half an hour. The formed white solid products were dried under vacuum overnight. The final material was denoted as pnm.

Compound **1**: 10 mL methanol solution of pnm (0.225 g, 1.3 mmol) was added at room temperature into a 10 mL methanol solution containing iron(II) chloride tetrahydrate (0.100g, 0.5 mmol), ammonium thiocyanate (0.076 g, 1.0 mmol) and ascorbic acid (0.030 g). The mixture was stirred for 5 minutes and the color of solution changed from limpid to yellow. The resulting solution was then kept for 2 hours to give large yellow crystals of **1**. (0.161 g, yield = 52 %). FTIR (KBr pellets): 562, 591, 624, 690, 752, 763, 1023, 1061, 1170, 1226, 1291, 1310, 1384, 1448, 1525, 1574, 1600, 1619, 2068, 3104, 3432. Elemental analysis calcd (%) for **1** (C₄₉H₄₀N₂₄S₄Fe₂): C 48.84, H 3.34, N 27.89, S 10.64; found: C 48.82, H 3.35, N 27.90, S 10.64.

3. Theoretical Calculations

Methodology

Various density functional theory (DFT) approaches, including a series of pure functionals (BP86, PW91, PBE, and M11-L), popular hybrid functionals (B3LYP, PBE1PBE, M06), and long range corrected functionals (HSEH1PBE, ω B97X, and LC- ω PBE), have been evaluated based on the experimental structure of dinuclear Fe(II) complex in the low-spin state, in order to determine a suitable functional for TD-DFT and DFT calculations on these systems. All DFT calculations are carried out with the Gaussian 09 program.¹ Here the LanL2DZ basis set augmented with polarization functions (Fe(ζ f)=2.462 and S(ζ d)=0.421)² is chosen to describe Fe and S atoms, and

the basis set of 6-311G(d,p) and TZVP are used for all other atoms. Moreover, the solvent effect is evaluated by the SMD³ model with the experimental methanol solvent. According to the calculated results in Table S4, it is noted that the effect of basis sets is not obvious, and the solvent-phase geometries could not coincide exactly with the crystal structure owing to the neglect of crystal packing effects and unattainable low-temperature conditions. Overall, the PBE1PBE-optimized structures show better agreement with the experimental data, compared to other methods. In consideration of computational costs, the PBE1PBE functional and the 6-311G(d,p) basis set have been used thoroughly here.

Confirmation of Spin Multiplicity for the High-Spin State

Due to the uncertainty of spin multiplicity for the high-spin state, the five possible structures with different spin multiplicities have been optimized at the PBE1PBE/6-311G(d,p) level, and the solvent effect was considered in calculation. Comparing the experimental and optimized average bond lengths of metal-ligand (Fe-N) and metal-metal (Fe-Fe) bonds, we note that the bond distances increase with the spin density, and when the spin multiplicity is set to 9, the corresponding optimized bond lengths match the crystal structure very well, suggesting that the high-spin state observed in experiment should have eight identical spin electrons ($S = 4$).

Electronic Absorption Spectrum

Herein TD-DFT calculations with the PBE1PBE functional are used for determination of the

electronic excitation energies and corresponding oscillator strengths. The solvent effect is taken into account by the SMD model in all the calculations. Since the excitation process is extremely faster than the movement of solvent molecules, the linear-response calculations with non-equilibrium solvation are performed to obtain the vertical excitation energies at the S_0 structure. The calculated excitation energies and oscillation strengths are compiled into Table S3, and the related absorption spectra and molecular orbitals for the $S_0 \rightarrow S_1$ transitions are displayed in Figures S4-S8. Calculations indicate that the absorption spectrum is in good agreement with the experimental observation for the high-spin state. Accordingly, the absorption at 288 nm is mainly contributed by the HOMO-LUMO $^1(\pi\pi^*)$ excitation, and the electronic transition at 341 nm is derived from $\pi(\text{SCN})$ to the $\pi^*(\text{pnm})$ (LLCT).

4. Additional Tables

Table S1. Elemental analyses.

	Elemental analysis (%)			
	N	C	H	S
1	27.90	48.82	3.35	10.64
ppm	32.53	62.77	4.68	

Table S2. Crystal data and structure refinement for **1** at 85, 100 and 230 K.

<i>T</i> / K	85	100	230
empirical formula	C ₅₃ H ₅₆ Fe ₂ N ₂₄ O ₄ S ₄		
Fw	1333.16		
crystal system	triclinic		
space group	<i>P</i> -1		
<i>a</i> / Å	12.2513(4)	12.2420(4)	12.3866(4)
<i>b</i> / Å	13.8462(4)	13.8866(4)	14.0248(6)
<i>c</i> / Å	21.0574(5)	21.0235(6)	21.2733(6)
α / °	104.407(3)	104.649(2)	105.519(3)
β / °	94.583(2)	94.761(3)	94.916(2)
γ / °	108.383(3)	108.177(3)	108.160(3)
Volume / Å ³	3234.07(18)	3233.91(18)	3325.3(2)
<i>Z</i>	2	2	2
ρ_{calc} / g cm ⁻³	1.237	1.237	1.203
μ / mm ⁻¹	5.223	5.224	5.080
<i>F</i> (000)	1236.0	1236.0	1236.0
Crystal size / mm ³	0.20 × 0.15 × 0.10		
Radiation	CuK α (λ = 1.54178)	CuK α (λ = 1.54178)	CuK α (λ = 1.54178)
2 Θ range for data collection/°	7.028 to 131.096	7.1 to 147.278	6.098 to 131.79
Reflections collected	19121	21767	20713
unique	R _{int} = 0.0377	R _{int} = 0.0489	R _{int} = 0.0434
Goodness-of-fit on F ²	1.091	1.060	1.118
Final R indexes [<i>I</i> ≥ 2 σ (<i>I</i>)]	R ₁ = 0.0717 wR ₂ = 0.1956	R ₁ = 0.0819 wR ₂ = 0.2174	R ₁ = 0.0662 wR ₂ = 0.1698
Final R indexes [all data]	R ₁ = 0.0851 wR ₂ = 0.2069	R ₁ = 0.1026 wR ₂ = 0.2283	R ₁ = 0.0927 wR ₂ = 0.1770
Largest diff. peak/hole / e Å ⁻³	2.46/-1.74	1.91/-0.76	0.70/-0.52

Table S3. Comparative analysis of selected bond lengths [\AA] between experimental data and theoretical calculation of **1**.

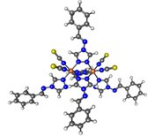
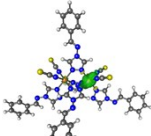
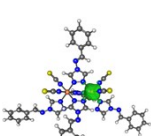
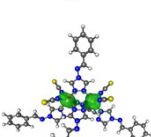
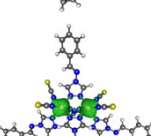
T/K	Experimental data			Theoretical calculations	
	85	100	230	LS	HS
Fe1-NCS	2.022(5)	2.047(6)	2.116(5)	1.955(4)	2.117(5)
Fe1-pnm	2.068(4)	2.093(5)	2.196(5)	1.978(4)	2.224(4)
Fe2-NCS	2.021(5)	2.032(5)	2.114(5)	1.954(5)	2.118(4)
Fe2-pnm	2.062(4)	2.075(4)	2.187(5)	1.978(4)	2.224(4)
Fe \cdots Fe	3.777	3.804	3.968	3.623	3.997

Table S4. Selected metal-ligand and metal-metal bond distances in the optimized geometries of low-spin state of **1** by different DFT approaches and the experiment (The temperature is set to 100 K).

Functional	Average bond length (\AA)			
	Fe-N1 ^a	Fe-N2 ^b	Fe-N3 ^c	Fe1-Fe2
	6-311G(d,p)/TZVP P	6-311G(d,p)/TZVP	6-311G(d,p)/TZVP	6-311G(d,p)/TZVP
Local				
BP86	1.929 / 1.927	1.968 / 1.973	1.948 / 1.951	3.615 / 3.619
PW91	1.923 / 1.924	1.962 / 1.970	1.943 / 1.949	3.602 / 3.610
PBE	1.923 / 1.925	1.964 / 1.965	1.945 / 1.952	3.604 / 3.611
M11-L	1.9151 / 1.916	1.942 / 1.945	1.927 / 1.929	3.540 / 3.544
Hybrid				
B3LYP	1.982 / 1.984	2.020 / 2.027	2.006 / 2.014	3.678 / 3.749
PBE1PBE	1.954 / 1.956	1.987 / 1.992	1.975 / 1.981	3.626 / 3.623
M06	1.949 / 1.951	1.984 / 1.988	1.976 / 1.978	3.620 / 3.625
Range-separated				
HSEH1PBE	1.955 / 1.957	1.988 / 1.993	1.976 / 1.982	3.625 / 3.633
ω B97X	1.998 / 1.990	2.022 / 2.018	2.019 / 2.009	3.672 / 3.661
Exp.		1.983 ^d / 2.050 ^f		3.648 ^d / 3.773 ^f

N1^a, N2^b, N3^c refer to the ligand (NCS), the mono- and bi-dentate-chelating pnm, respectively. ^dThe experimental data at 77K in Reference⁴. ^fThe experimental data at 85 K.

Table S5. Selected metal-ligand and metal-metal average bond distances in the optimized geometries of different spin states of **1** by PBE1PBE and the available experimental values (The calculated temperature is 300K).

Spin multiplicity	Average bond length (Å)			Spin density
	Fe1-N ^a	Fe2-N ^b	Fe1-Fe2	
1	1.970	1.970	3.623	
3	1.975	2.079	3.727	
5	1.978	2.178	3.833	
7	2.092	2.184	3.922	
9	2.189	2.189	3.997	
Exp. (HS)	2.180 ^c / (2.153 & 2.156) ^d		3.966 ^c / 3.938 ^d	

Fe1-N^a and Fe2-N^b refer to the average bond length between Fe center with N atoms of ligands. ^cReference⁴. ^d The experimental data at 230 K.

Table S6. The predicted excitation energies (E/λ), corresponding oscillator strengths (f), and assignment for the lowest 60 transitions of **1** in the high-spin and low-spin states by TD-PBE1PBE (the LanL2DZ pseudo-potentials for Fe and S and the 6-311G(d,p) basis set for all other atoms).

High-spin				Low-spin			
E (eV)	λ (nm)	f	Main configurations	E (eV)	λ (nm)	f	Main configurations

0.3183	3894.68	0.0000		2.2085	561.39	0.0000	
0.3230	3839.05	0.0001		2.2298	556.02	0.0000	
0.4186	2962.01	0.0000		2.2611	548.34	0.0001	
0.4258	2911.46	0.0000		2.2731	545.45	0.0000	
1.6585	747.56	0.0000		2.2922	540.91	0.0003	
1.6722	741.43	0.0000		2.3028	538.40	0.0001	
1.8043	687.16	0.0000		3.1307	396.03	0.0190	
1.8114	684.45	0.0000		3.1349	395.49	0.0072	
2.7874	444.80	0.0000		3.1590	392.47	0.0224	H → L+1 (0.31) H → L (0.27)
2.7920	444.07	0.0000		3.1764	390.32	0.0036	
2.7979	439.67	0.0000		3.1959	387.95	0.0026	
2.8200	438.90	0.0000		3.2055	386.78	0.0037	
2.8249	385.40	0.0006		3.2149	385.65	0.0033	
3.2170	384.36	0.0006		3.2236	384.61	0.0303	H-2 → L (0.34) H-1 → L+1 (0.24)
3.2257	380.93	0.0027	274B→277B (0.64) 275B→ 277B (0.38)	3.2311	383.72	0.0098	
3.2548	380.84	0.0021	274B→277B (0.48) 275B→ 278B (0.29)	3.2390	382.78	0.0065	
3.2555	376.41	0.0006		3.2485	381.66	0.0121	
3.2939	375.92	0.0004		3.2586	380.49	0.0090	
3.2981	372.83	0.0023	274B→278B (0.82)	3.2627	380.00	0.0013	
3.3255	370.72	0.0009		3.2774	378.30	0.0135	
3.3444	351.93	0.0000		3.2798	378.02	0.0033	
3.5230	350.68	0.0000		3.2858	377.33	0.0152	
3.5356	345.85	0.0002		3.3027	375.40	0.0137	
3.5849	342.26	0.0003		3.3172	373.76	0.0060	
3.6225	342.07	0.0002		3.3277	372.58	0.0013	
3.6246	341.50	0.0028	273B→276B (0.65)	3.3325	372.05	0.0054	
3.6306	339.69	0.0001		3.3426	370.92	0.0037	
3.6499	339.39	0.0001		3.3509	370.00	0.0098	
3.6531	338.24	0.0006		3.3558	369.47	0.0008	
3.6656	338.06	0.0001		3.3628	368.69	0.0106	
3.6675	336.53	0.0012		3.3701	367.89	0.0068	
3.6842	336.45	0.0001		3.3874	366.01	0.0122	
3.6851	336.15	0.0001		3.3961	365.08	0.0051	
3.6883	335.56	0.0001		3.4150	363.06	0.0080	
3.6949	335.19	0.0002		3.4273	361.76	0.0079	
3.6989	335.12	0.0001		3.4302	361.45	0.0053	

3.6996	334.87	0.0004	3.4782	356.46	0.0001	
3.7025	334.36	0.0001	3.4846	355.81	0.0000	
3.7082	333.86	0.0002	3.4961	354.63	0.0000	
3.7137	333.06	0.0001	3.5158	352.65	0.0007	
3.7225	332.95	0.0001	3.5425	349.99	0.0003	
3.7238	332.33	0.0002	3.5508	349.17	0.0032	
3.7308	331.73	0.0002	3.5585	348.42	0.0013	
3.7375	331.52	0.0006	3.5671	347.58	0.0007	
3.7398	330.67	0.0003	3.5689	347.40	0.0008	
3.7494	329.69	0.0001	3.5774	346.57	0.0004	
3.7606	329.28	0.0001	3.6050	343.93	0.0000	
3.7653	328.57	0.0002	3.6131	343.16	0.0003	
3.7734	327.93	0.0000	3.6239	342.12	0.0000	
3.7808	327.82	0.0008	3.6341	341.17	0.0001	
3.7821	327.54	0.0001	3.7887	327.24	0.0001	
3.7853	327.15	0.0001	3.8066	325.71	0.0002	
3.7899	326.69	0.0002	3.9375	314.88	0.1023	H-8 → L+1 (0.62)
3.7951	325.27	0.0001	3.9502	313.86	0.0270	
3.8117	325.03	0.0007	3.9841	311.20	0.0837	H-9 → L+1 (0.42) H-8 → L+3 (0.30)
3.8145	324.48	0.0001	3.9929	310.51	0.0693	
3.8210	324.20	0.0004	4.0206	308.37	0.0180	
3.8243	324.12	0.0013	4.0305	307.62	0.0557	
3.8253	323.57	0.0003	4.0533	305.89	0.0360	
3.8317	326.69	0.0002	4.0719	304.48	0.0087	

Table S7. Optimized geometries of **1** in the high-spin state.

HS					
Atom	Elem.	X coord.	Y coord.	Z coord.	
1	C	-4.52491300	-1.21561900	0.01884500	
2	H	-5.19944400	-0.45073600	-0.33192700	
3	C	-3.73255500	-3.10663600	0.70876400	
4	H	-3.70374800	-4.13252300	1.04228300	
5	C	-7.13886600	-2.33783000	0.58429500	
6	H	-7.05332600	-1.25817700	0.72299200	
7	C	-8.48552900	-2.89081400	0.59259400	
8	C	-8.73575300	-4.25111700	0.36798700	
9	H	-7.90661600	-4.92210000	0.17126400	

10	C	10.03541600	-4.72763000	0.39326400
11	H	10.22768800	-5.78103500	0.21751800
12	C	11.09756200	-3.85728900	0.63940800
13	H	12.11451500	-4.23613200	0.65610700
14	C	10.85634700	-2.50591600	0.85951200
15	H	11.68193200	-1.82799800	1.04916500
16	C	-9.55456100	-2.02262100	0.83498300
17	H	-9.35859600	-0.96818400	1.00547200
18	C	0.96199200	3.67650900	-1.22749100
19	H	1.98074200	4.01706800	-1.32241100
20	C	-1.20176300	3.62667200	-1.26245800
21	H	-2.22739900	3.94525600	-1.36405300
22	C	0.67156400	6.54748600	-1.44371200
23	H	1.50119600	6.20971400	-0.81849300
24	C	0.67231800	7.95279300	-1.81981300
25	C	-0.30608400	8.50309600	-2.65852000
26	H	-1.09023400	7.86809700	-3.05616300
27	C	-0.26394700	9.84987300	-2.97613500
28	H	-1.02172800	10.27507400	-3.62611600
29	C	0.75074400	10.66010700	-2.46602700
30	H	0.77870000	11.71508300	-2.71970400
31	C	1.72682200	10.11927700	-1.63677400
32	H	2.51737100	10.74838400	-1.24131300
33	C	1.68955600	8.76895700	-1.31511800
34	H	2.44807400	8.33812900	-0.66814200
35	C	1.08870800	-1.52717600	-2.44573500
36	H	2.11934000	-1.73823300	-2.67918500
37	C	-1.07545800	-1.55116000	-2.45689200
38	H	-2.09009600	-1.81886300	-2.70619000
39	C	0.92534600	-3.84928600	-4.18475100
40	H	1.87086100	-3.71598300	-3.65598500
41	C	0.89312500	-4.89943300	-5.19227200
42	C	-0.25322400	-5.17423600	-5.94991700
43	H	-1.15348500	-4.59101000	-5.79009800
44	C	-0.22924100	-6.18419000	-6.89642800
45	H	-1.11765000	-6.39527700	-7.48271600
46	C	0.93292200	-6.92889500	-7.09947300
47	H	0.94575000	-7.71792700	-7.84480700
48	C	2.07367300	-6.66107800	-6.35142300
49	H	2.97838600	-7.23869000	-6.50956500

50	C	2.05502000	-5.64931200	-5.40025100
51	H	2.94276200	-5.43352000	-4.81315900
52	C	3.93914300	-2.84486300	0.75195600
53	H	3.96432500	-3.89627400	0.98950100
54	C	4.57076000	-0.81325900	0.35586000
55	H	5.19776600	0.05757000	0.24552600
56	C	6.68157600	-3.29926800	1.62640400
57	H	5.93794000	-4.00515000	2.00065400
58	C	8.07334900	-3.61653000	1.91622600
59	C	9.13172400	-2.80624100	1.48422800
60	H	8.92120400	-1.91350400	0.90537100
61	C	10.43627400	-3.14849500	1.79739400
62	H	11.25431600	-2.51918300	1.46210900
63	C	10.70173500	-4.29877800	2.54064400
64	H	11.72661100	-4.56167600	2.78272200
65	C	9.65660300	-5.10863600	2.96995700
66	H	9.86148000	-6.00433400	3.54706200
67	C	8.34617200	-4.76959200	2.65884600
68	H	7.52489400	-5.39749900	2.99186800
69	C	-1.07354500	0.06777800	2.54756600
70	H	-2.09478800	-0.03577500	2.87763200
71	C	1.09019100	0.09682700	2.53304400
72	H	2.11226200	0.04539500	2.87349000
73	C	-0.82283900	-0.00228500	5.43425400
74	H	-1.68168500	0.55470100	5.05359200
75	C	-0.82144200	-0.29946200	6.85837000
76	C	0.20496000	-1.03299600	7.46832100
77	H	1.02831000	-1.40410200	6.86778500
78	C	0.16087900	-1.28008300	8.82967200
79	H	0.95622200	-1.84774300	9.30152000
80	C	-0.90328100	-0.80302900	9.59541800
81	H	-0.93252200	-1.00127200	10.66217800
82	C	-1.92616700	-0.07699800	8.99585400
83	H	-2.75438300	0.29328100	9.59087700
84	C	-1.88689000	0.17408900	7.63065600
85	H	-2.68158300	0.74023900	7.15360900
86	C	-3.80522800	2.25947900	1.81972800
87	C	-3.89618800	1.05828800	-3.10791700
88	C	3.72572500	1.23501800	-3.17862500
89	C	3.51576300	3.07049900	1.31105700

90	N	-3.22356900	-1.11534500	0.10691200
91	N	-2.71829200	-2.30560600	0.55028100
92	N	-4.89263800	-2.46494400	0.40137900
93	N	-6.11651100	-3.09190500	0.43437700
94	N	0.58168500	2.46325700	-0.93060300
95	N	-0.77959800	2.43256400	-0.94439700
96	N	-0.13856000	4.44600800	-1.43594100
97	N	-0.26642300	5.76246800	-1.82105800
98	N	0.66915600	-0.61140000	-1.61556300
99	N	-0.69174100	-0.62853000	-1.61798500
100	N	0.01164400	-2.15133200	-2.99563200
101	N	-0.11090300	-3.13931200	-3.94417500
102	N	2.87963800	-2.16977200	0.40941500
103	N	3.27998200	-0.88496800	0.16611000
104	N	5.03492100	-2.02441600	0.73699700
105	N	6.36969600	-2.24115100	0.98001400
106	N	-0.68149200	0.31019400	1.32571500
107	N	0.67884200	0.33638600	1.31707200
108	N	0.01967600	-0.06446300	3.34407100
109	N	0.14444800	-0.37037400	4.68126400
110	N	-3.22217600	1.84620400	0.88601900
111	N	-3.22308800	0.95151600	-2.15014100
112	N	3.07760700	1.10404000	-2.20639700
113	N	3.08777700	2.12655600	0.75628100
114	S	-4.61504300	2.83430900	3.12827200
115	S	-4.83594100	1.21168000	-4.44649900
116	S	4.63358300	1.41789800	-4.53381500
117	S	4.10996100	4.39264400	2.08679900
118	Fe	-2.03343000	0.67984800	-0.42199800
119	Fe	1.96236600	0.77918000	-0.44979900

Table S8. Optimized geometries of **1** in the low-spin state.

Atom	Elem.	X coord.	Y coord.	Z coord.
1	C	4.18538300	-1.26216600	0.41668700
2	H	4.88248800	-0.46169000	0.59879900
3	C	3.31919900	-3.22714800	0.14450000
4	H	3.24850600	-4.29877600	0.04036100
5	C	6.75974800	-2.57406100	0.20570500

6	H	6.73962400	-1.52067600	-0.08033500
7	C	8.07467700	-3.18982400	0.31482000
8	C	8.24425900	-4.53332300	0.67524600
9	H	7.37412600	-5.14455900	0.88864300
10	C	9.51741400	-5.07103100	0.75702300
11	H	9.64689700	-6.11185100	1.03546000
12	C	10.63312000	-4.27889200	0.48511500
13	H	11.62874900	-4.70568600	0.55305000
14	C	10.47207400	-2.94476100	0.12916700
15	H	11.33903800	-2.32757400	-0.08210900
16	C	9.19696500	-2.40104700	0.04355900
17	H	9.06290500	-1.35946200	-0.23341500
18	C	-0.84357700	3.60831000	0.40184900
19	H	-1.84852000	3.99407900	0.37604800
20	C	1.31216000	3.46078700	0.59238400
21	H	2.34581400	3.73709200	0.72076200
22	C	-0.43458400	6.47148800	0.34804700
23	H	-1.31352700	6.10921300	-0.18891400
24	C	-0.34471800	7.91041800	0.54482900
25	C	0.70843200	8.50467400	1.25291000
26	H	1.48751500	7.88152100	1.67835900
27	C	0.74610700	9.87980300	1.40797800
28	H	1.56158500	10.33890900	1.95727200
29	C	-0.26191700	10.67568000	0.86325200
30	H	-0.22800900	11.75307400	0.99052500
31	C	-1.31034900	10.09215600	0.16101500
32	H	-2.09515000	10.71041300	-0.26206600
33	C	-1.35322100	8.71322800	0.00244800
34	H	-2.16918100	8.24924800	-0.54374100
35	C	-1.34268700	-0.83451600	2.44618100
36	H	-2.39782800	-0.91703400	2.64429700
37	C	0.81206800	-0.96719900	2.64437900
38	H	1.78514800	-1.21357300	3.03553200
39	C	-1.44701900	-2.71384100	4.65084500
40	H	-2.30590100	-2.72237500	3.97717800
41	C	-1.57815800	-3.48617100	5.87710800
42	C	-0.56491700	-3.53180000	6.84399400
43	H	0.35025700	-2.97117600	6.68744200
44	C	-0.73947500	-4.28673800	7.99122900
45	H	0.04509200	-4.31952300	8.74021300

46	C	-1.92127300	-5.00152500	8.18827000
47	H	-2.05323800	-5.58967000	9.09090900
48	C	-2.93048200	-4.96020900	7.23292800
49	H	-3.85009500	-5.51523400	7.38606700
50	C	-2.76102800	-4.20394300	6.08065600
51	H	-3.54487100	-4.16569300	5.32985400
52	C	-3.70020700	-2.70877500	-0.50849300
53	H	-3.75347800	-3.78347100	-0.57855000
54	C	-4.28234500	-0.62535000	-0.41293600
55	H	-4.88567900	0.26764200	-0.42250300
56	C	-6.45197400	-3.21214100	-1.30413200
57	H	-5.71720400	-3.94794200	-1.63611500
58	C	-7.85176100	-3.55641300	-1.51049300
59	C	-8.89634500	-2.71187500	-1.11178900
60	H	-8.66794300	-1.77101600	-0.62295000
61	C	10.21027800	-3.08195600	-1.34297500
62	H	11.01778400	-2.42603500	-1.03426400
63	C	10.49882700	-4.29467100	-1.96919200
64	H	11.53107100	-4.57909400	-2.14712200
65	C	-9.46731500	-5.13890200	-2.36409300
66	H	-9.69002700	-6.08268700	-2.85087700
67	C	-8.14743900	-4.77205200	-2.13533200
68	H	-7.33622000	-5.42620300	-2.44141800
69	C	1.28796100	-0.48258200	-2.34581800
70	H	2.32294500	-0.69231500	-2.55696200
71	C	-0.86835000	-0.35222600	-2.52259400
72	H	-1.86222800	-0.41464700	-2.93357900
73	C	1.26065300	-1.11508000	-5.16603500
74	H	2.13495100	-0.56458000	-4.81289300
75	C	1.34590900	-1.67919300	-6.50414600
76	C	0.31065000	-2.43976600	-7.06403100
77	H	-0.58888000	-2.62784400	-6.48802300
78	C	0.44269100	-2.94691000	-8.34534500
79	H	-0.35977600	-3.53514300	-8.77831200
80	C	1.60398100	-2.70563000	-9.07984600
81	H	1.70138000	-3.10698100	10.08363300
82	C	2.63596600	-1.95445600	-8.52889700
83	H	3.53970700	-1.76704600	-9.09922100
84	C	2.50859600	-1.44256800	-7.24436800
85	H	3.30997400	-0.85431400	-6.80710800

86	C	3.95337400	1.84340400	-1.58130000
87	C	3.52471500	1.50815600	2.81677400
88	C	-3.69216700	2.01106400	2.16681500
89	C	-3.22130700	2.49676300	-2.13797100
90	N	2.88839200	-1.13942600	0.28831700
91	N	2.33609300	-2.37351100	0.11044700
92	N	4.50138500	-2.57940600	0.32227900
93	N	5.69615500	-3.24987300	0.42511800
94	N	-0.50949400	2.34828300	0.30660800
95	N	0.83939100	2.25516100	0.41977700
96	N	0.28632300	4.34302100	0.57484900
97	N	0.48196400	5.68920000	0.77841900
98	N	-0.79947400	-0.18543200	1.44973000
99	N	0.54987200	-0.27334600	1.56906800
100	N	-0.35062900	-1.35189200	3.21768000
101	N	-0.37118000	-2.07332400	4.38808800
102	N	-2.61808400	-2.01534300	-0.29289900
103	N	-2.98810200	-0.70380900	-0.24161500
104	N	-4.77577500	-1.87032800	-0.59765700
105	N	-6.11971700	-2.09705400	-0.77357600
106	N	0.81513800	0.00032100	-1.22625900
107	N	-0.53387900	0.08927600	-1.33865200
108	N	0.25036700	-0.71087500	-3.19139400
109	N	0.20573600	-1.25402800	-4.45495900
110	N	3.16686000	1.38005000	-0.84769200
111	N	2.90670500	1.12658700	1.89810900
112	N	-2.95038800	1.54925400	1.38705200
113	N	-2.67455400	1.83164600	-1.34432900
114	S	5.06037800	2.48926400	-2.62103900
115	S	4.38954400	2.04776700	4.11445200
116	S	-4.73755800	2.66034500	3.26613200
117	S	-3.98939100	3.43325000	-3.25878400
118	Fe	1.85977200	0.55706200	0.35013500
119	Fe	-1.74037500	0.81691800	0.03909700

5. Additional Figures

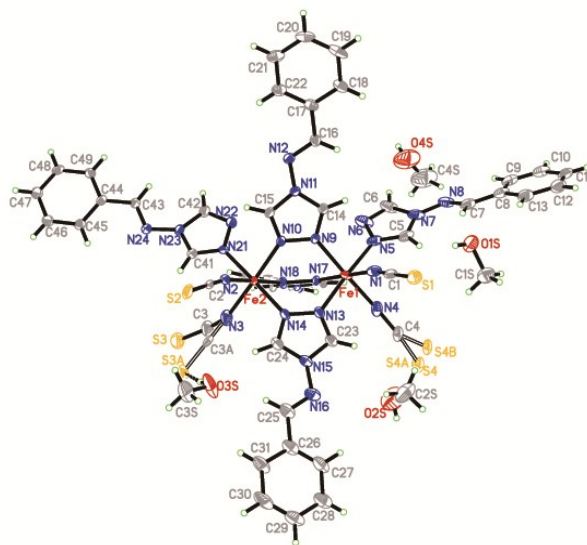


Figure S1. ORTEP drawing of the molecular structure of 1, lattice methanol molecules are omitted for clarity.

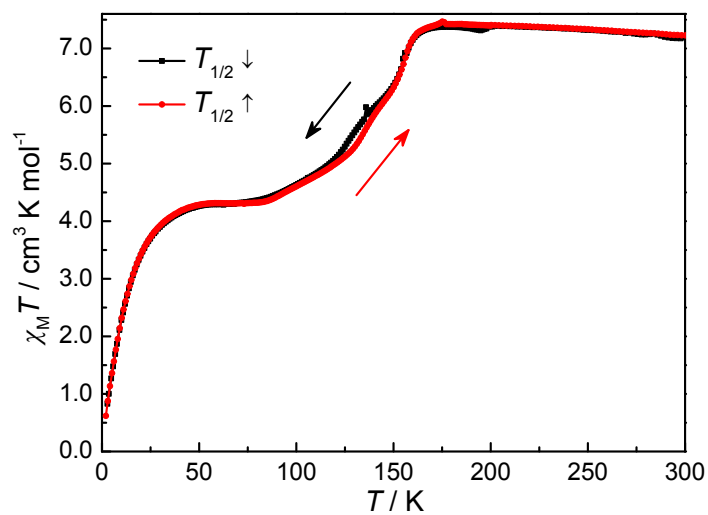


Figure S2. Magnetic properties 1 under applied field of 5000 Oe, sweeping rate: 1 K mol⁻¹.

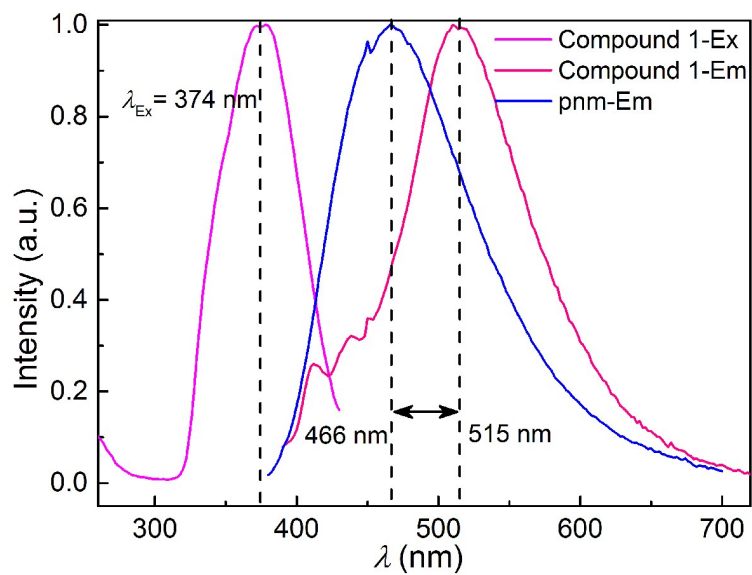


Figure S3. Solid-state fluorescence spectra of **1** and pnm at room temperature. Excitation: 347 nm for pnm, 374 nm for **1**. Em: emission.

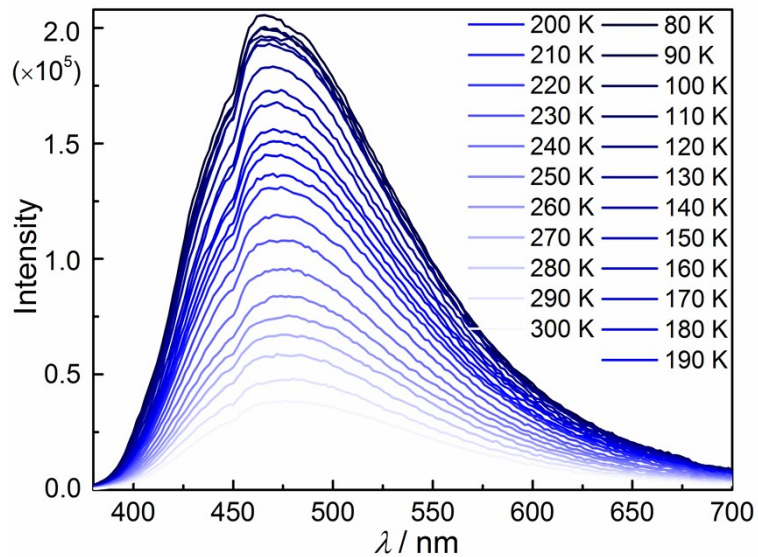
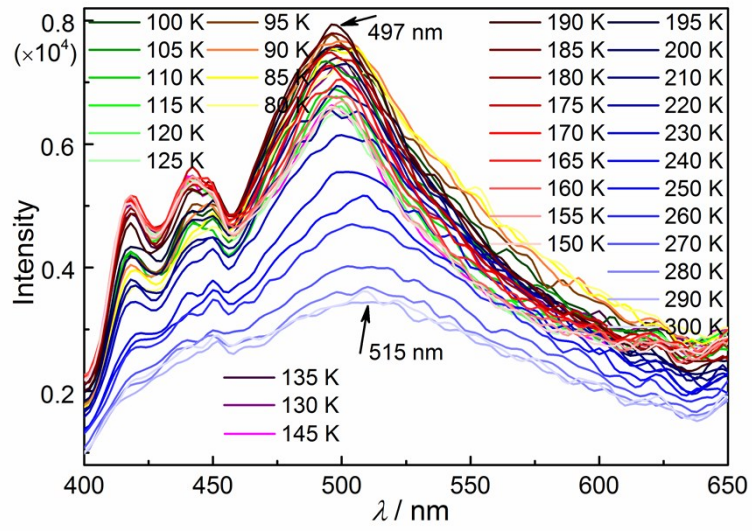
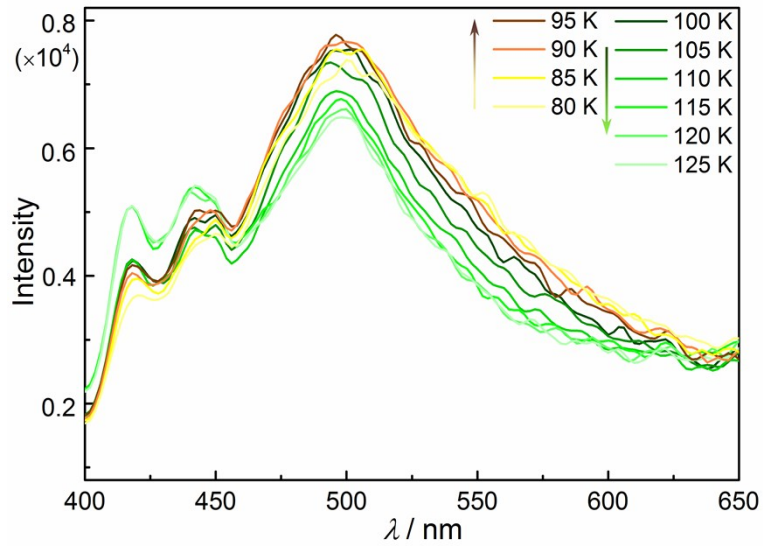


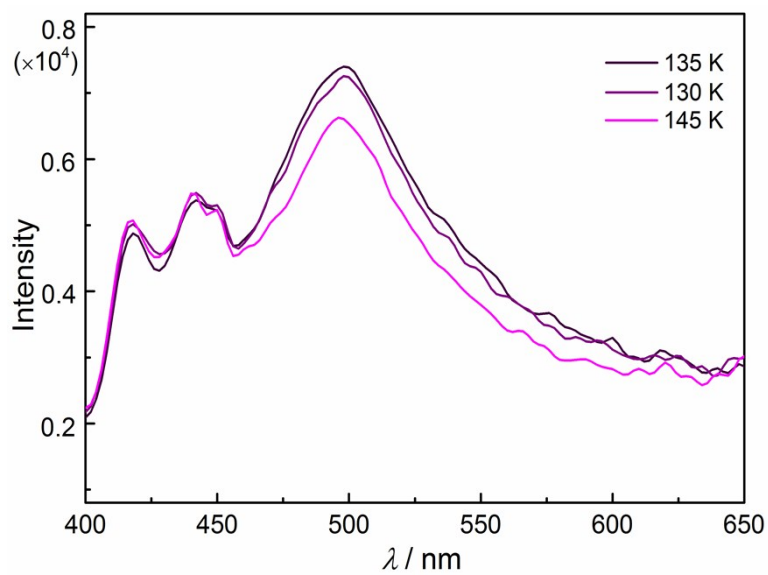
Figure S4. Temperature-dependent fluorescent emission spectra of pnm in the solid states.



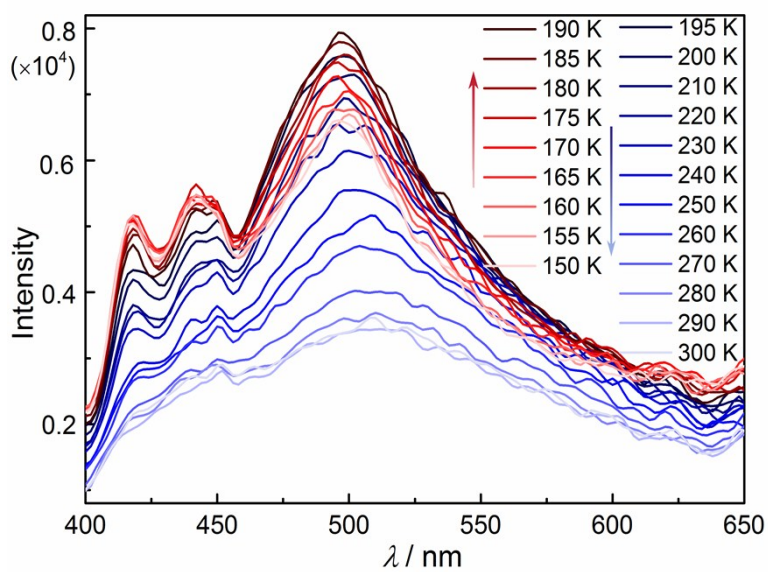
(a)



(b)



(c)



(d)

Figure S5. (a) Temperature-dependent fluorescent emission spectra of **1** in the solid states (80-300 K). (b) Temperature-dependent fluorescent emission spectra of **1** in the solid states (80-125 K). The

arrow indicates the trend of emission intensity with increasing temperature. (c) Temperature-dependent fluorescent emission spectra of **1** in the solid states (130-145 K). The arrow indicates the trend of emission intensity with increasing temperature. (d) Temperature-dependent fluorescent emission spectra of **1** in the solid states (150-300 K). The arrow indicates the trend of emission intensity with increasing temperature.

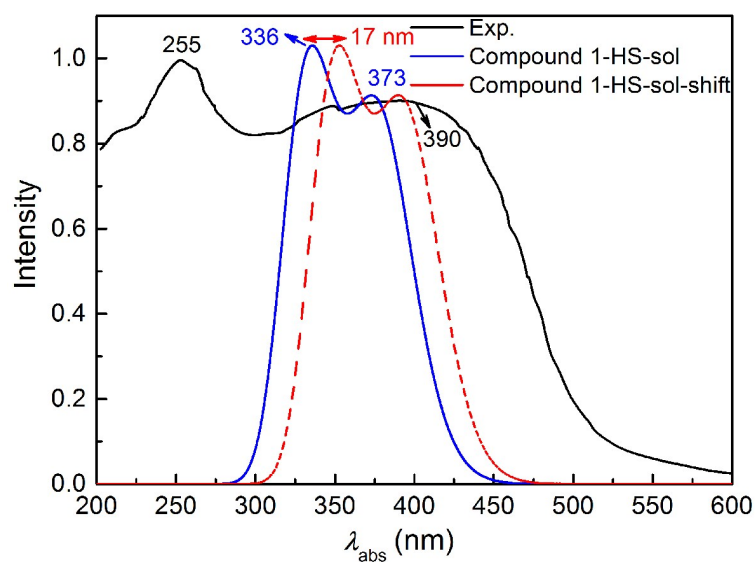


Figure S6. Experimental spectrum and electronic absorption spectra predicted by TD-PBE1PBE in methanol solvent for the high-spin state **1**. (Gaussian HFWD is set to 0.333 eV).

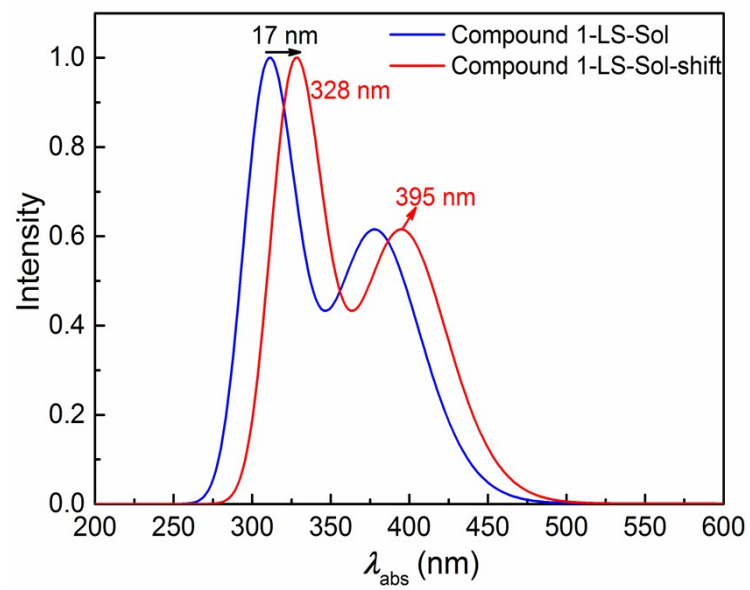


Figure S7. Electronic absorption spectra predicted by TD-PBE1PBE in methanol solvent for the low-spin state of **1**. (Gaussian HFWD is set to 0.333 eV).

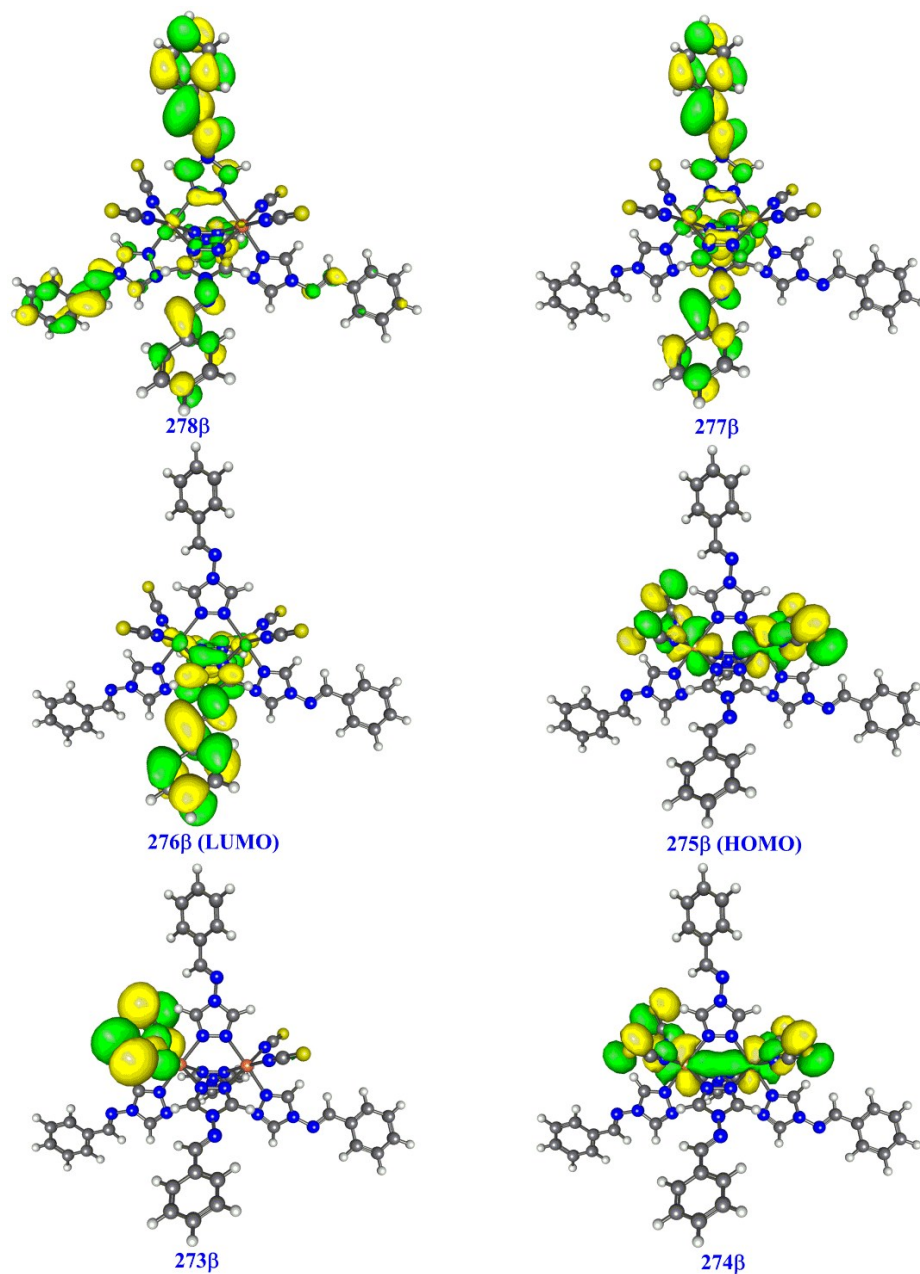


Figure S8. Selected key molecular orbitals of the $S_0 \rightarrow S_1$ transition for the high-spin state. (no alpha-spin electron contribution, isovalue : 0.05 a.u.)

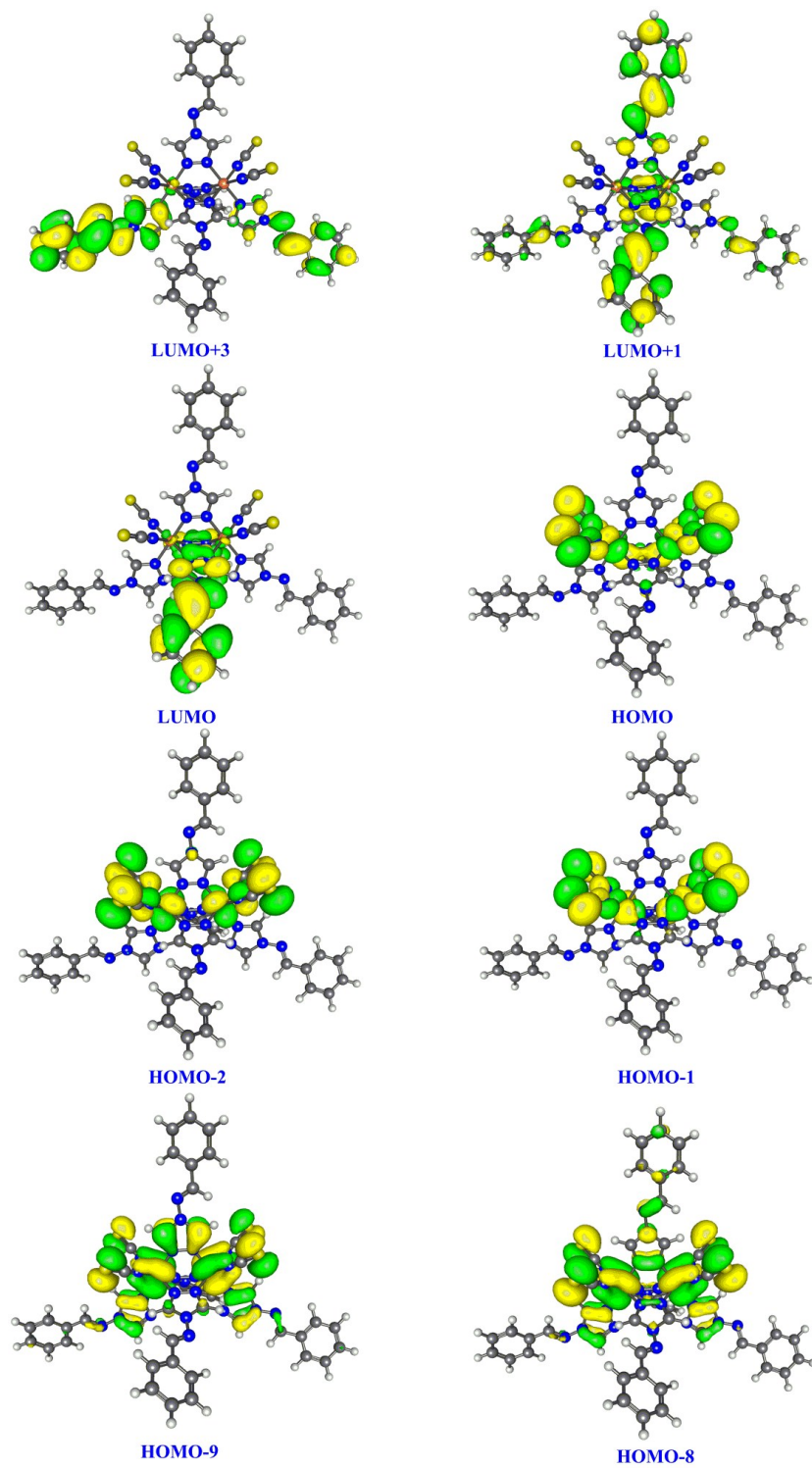


Figure S9. Selected key molecular orbitals of the $S_0 \rightarrow S_1$ transition for the low-spin state. (isovalue : 0.05 a.u.).

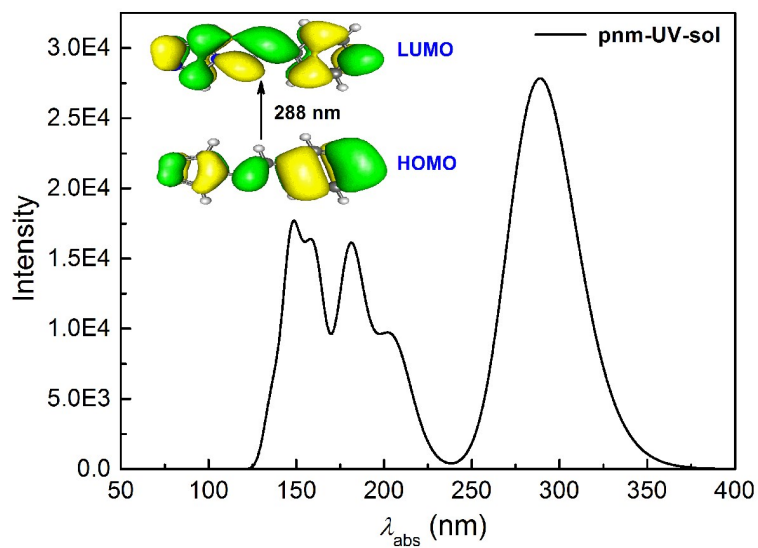


Figure S10. Electronic absorption spectrum calculated by TD-PBE1PBE in methanol solvent for the ligand pnm. (Gaussian HFWD is set to 0.200 eV).

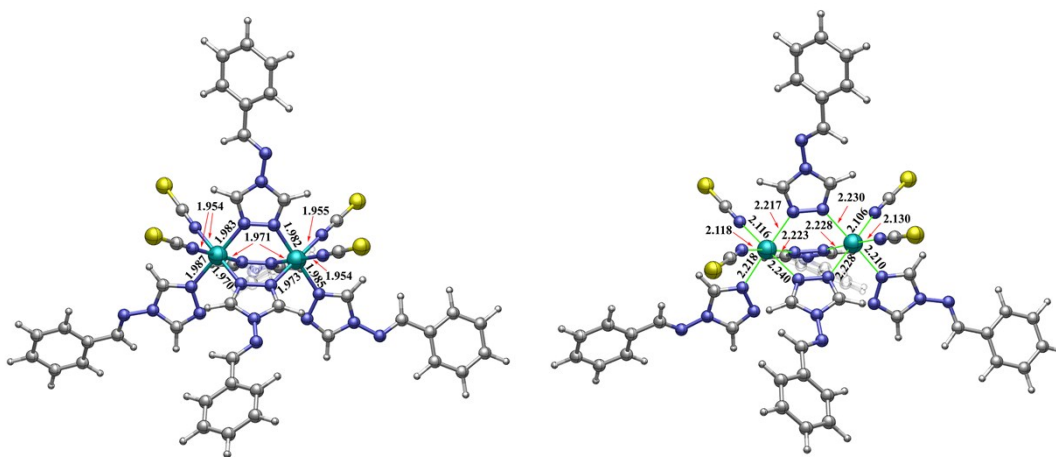


Figure S11. Left: crystal structure of **1** in the LS state obtained by theoretical calculation. Right: crystal structure of **1** in the HS state obtained by theoretical calculation.

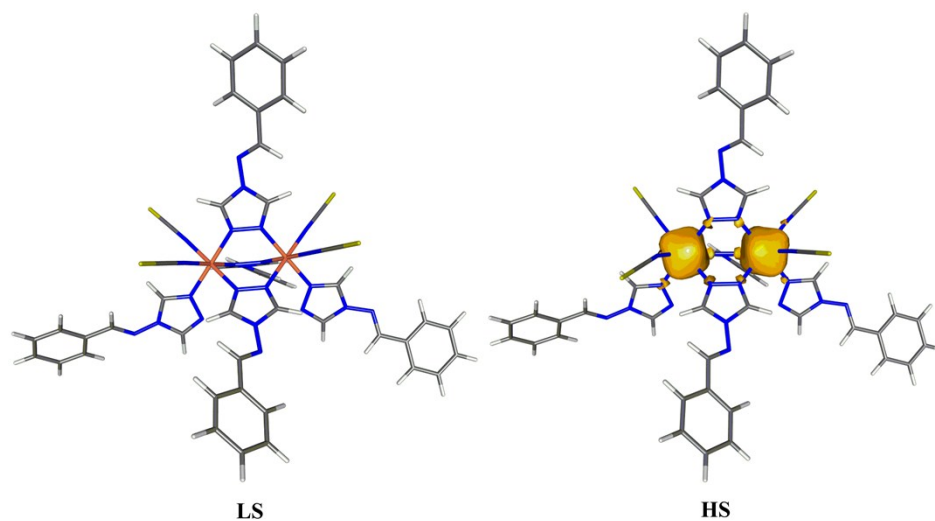


Figure S12. The electronic spin density of **1** in the HS state and in the LS state, respectively, which were obtained by theoretical calculation.

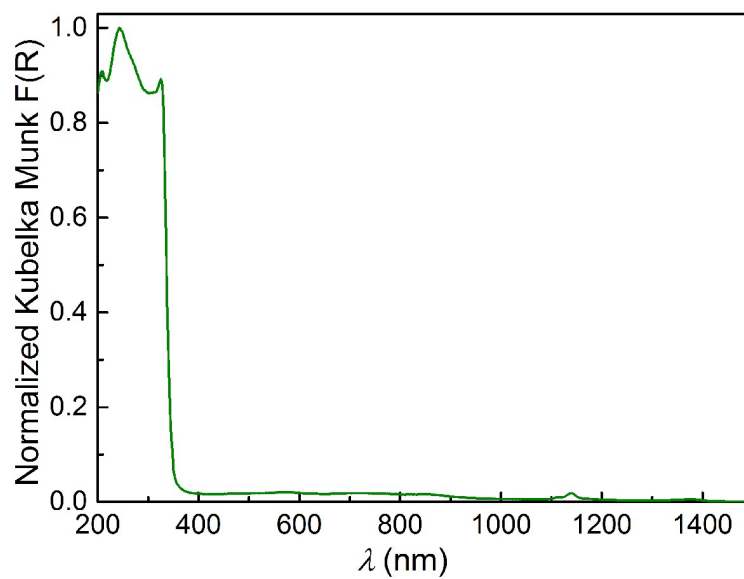


Figure S13. The normalized diffuse reflectivity spectra (DRS) of pnm.

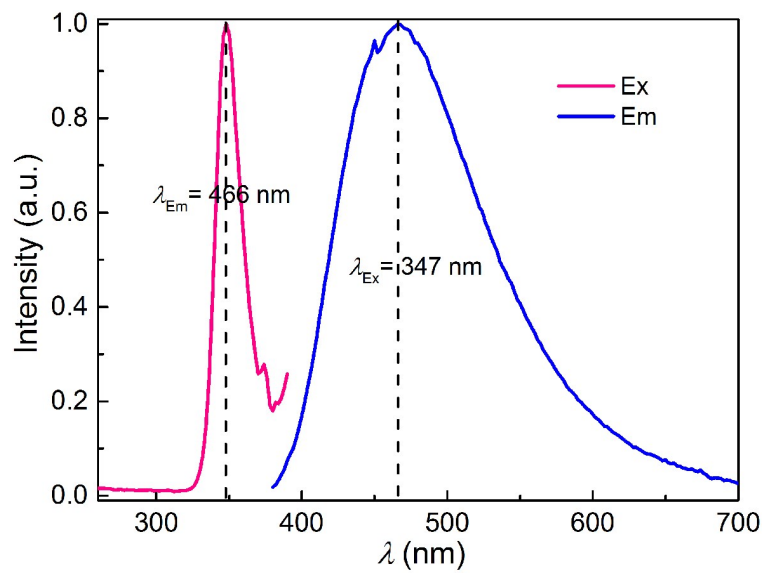


Figure S14. Normalized excitation spectra and emission spectra of pnm ($\lambda_{\text{ex}} = 347$ nm and $\lambda_{\text{em}} = 466$ nm).

6. REFERENCES

- (1) Frisch, M. J.; Trucks, G. W.; Schlegel, H. B.; Scuseria, G. E.; Robb, M. A.; Cheeseman, J. R.; Scalmani, G.; Barone, V.; Mennucci, B.; Petersson, G. A.; Nakatsuji, H.; Caricato, M.; Li, X.; Hratchian, H. P.; Izmaylov, A. F.; Bloino, J.; Zheng, G.; Sonnenberg, J. L.; Hada, M.; Ehara, M.; Toyota, K.; Fukuda, R.; Hasegawa, J.; Ishida, M.; Nakajima, T.; Honda, Y.; Kitao, O.; Nakai, H.; Vreven, T.; Montgomery, J. A., Jr.; Peralta, J. E.; Ogliaro, F.; Bearpark, M.; Heyd, J. J.; Brothers, E.; Kudin, K. N.; Staroverov, V. N.; Kobayashi, R.; Normand, J.; Raghavachari, K.; Rendell, A.; Burant, J. C.; Iyengar, S. S.; Tomasi, J.; Cossi, M.; Rega, N.; Millam, J. M.; Klene, M.; Knox, J. E.; Cross, J. B.; Bakken, V.; Adamo, C.; Jaramillo, J.; Gomperts, R.; Stratmann, R. E.; Yazyev, O.; Austin, A. J.; Cammi, R.; Pomelli, C.; Ochterski, J. W.; Martin, R. L.; Morokuma, K.; Zakrzewski, V. G.; Voth, G. A.; Salvador, P.; Dannenberg, J. J.; Dapprich, S.; Daniels, A. D.; Farkas, O.; Foresman, J. B.; Ortiz, J. V.; Cioslowski, J.; Fox, D. J. Gaussian 09, revision D.01; Gaussian, Inc. : Wallingford, CT, **2009**.
- (2) Ehlers A W, Böhme M, Dapprich S, Gobbi A, Höllwarth A, Jonas V, Köhler K F, Stegmann R, Veldkamp A, Frenking G. *Chem. Phys. Lett.* **1993**, *208*:111–114
- (3) Marenich, A. V.; Cramer, C. J.; Truhlar, D. G. *J. Phys. Chem. B* **2009**, *113*, 6378–6396.
- (4) Garcia, Y.; Robert, F.; Naik, A. D.; Zhou, G. Y.; Tinant, B.; Robeyns, K.; Michotte, S.; Piraux, L. *J. Am. Chem. Soc.* **2011**, *133*, 15850-15853